# Electrochemical Properties of $LiCo_{0.4}Ni_{0.6}O_2$ and its Performances in Rechargeable Lithium Batteries

## N.W.B. Balasooriya[1,*] and P.W.S.K. Bandaranayake[2]

*[1]Faculty of Applied Sciences, South Eastern University of Sri Lanka*
*[2]Department of Physics, University of Peradeniya, Peradeniya*

## ABSTRACT

Intercalation cathode materials belonging to the 4-volt class electrodes, lithiated cobalt oxide $LiCoO_2$ and lithiated nickel cobalt oxide $LiCo_{0.4}Ni_{0.6}O_2$, were synthesized by sol-gel technique. The structural characteristics of the compounds were studied using XRD, FTIR and DSC. The compounds were used as cathode materials for assembling rechargeable lithium-batteries and their electrochemical performances were studied. The potentiostat and galvanostat techniques were used to determine the electrochemical characteristics. The irreversible capacity loss of $LiCoO_2$ during the first charge-discharge is about 20% and for $LiCo_{0.4}Ni_{0.6}O_2$ is about 90% for two different current rates of 5 and 10 A $kg^{-1}$. The overall electrochemical capacity of $LiCo_{0.4}Ni_{0.6}O_2$ has been drastically reduced due to the *s*-block or *p*-block metal substitution. Also the un-reacted materials remained as impurities gave a very poor cycleability. However more stable charge-discharge performances have been observed for $LiCoO_2$ at different current rates. Differences and similarities between these two cathode materials in batteries are also discussed. The Li-ion batteries were assembled using the sol-gel synthesized cathode materials, natural untreated vein graphite of Sri Lanka as the anode material and 1 M $LiPF_6$ in EC/DMC as liquid electrolyte, and their performances were tested.

## 1. INTRODUCTION

Lithium cobalt oxide ($LiCoO_2$) is extensively used as a cathode material in commercially available Li-ion batteries due to its high energy density and good cycle-life performances.

---

* Corresponding author: balasooriya@seu.ac.lk

However its major drawbacks are high price and toxicity of cobalt. To overcome these problems, various cathode materials without cobalt, such as $LiM_xNi_yO_2$ where M is one of the transition or alkaline earth metals have been used. However the battery performances of $LiCoO_2$ are superior to other cathode materials. Therefore, the present study was focused to reduce the cost and toxicity of Co by replacing 60% of Co by a cheaper and non-toxic element Ni.

The electrochemical properties of cathode materials mainly depend on the structure and morphology of the materials characteristic to different synthesis methods. High temperature (HT) and low temperature (LT) synthesis are commonly used for solid state preparation of cathode materials. The HT preparation method produces larger particles with lower cell capacity, and LT preparation methods, such as sol-gel process using a complexing/chelating agent, produces fine particles with higher capacity [1, 2]. Lithium cobalt nickel oxides have also been synthesized by others using aqueous or alcoholic solution of various carboxylic acids [3, 4]. In the present study we have tried another widely used chelating agent, citric acid, for the synthesis of oxides.

The aim of the present work is to study the structural and electrochemical properties of $LiCoO_2$ and $LiCo_{0.4}Ni_{0.6}O_2$ synthesized by sol-gel method and testing the performances in the 4-volts class Li-ion batteries.

## 2. METHODOLOGY

Lithium nitrate, $LiNO_3$ and cobalt nitrate $Co(NO_3)_2.6H_2O$ and nickel nitrates, $Ni(NO_3)_2.6H_2O$ (all are analytical grade Merck products) were used as starting materials and they were dried at 120 °C for 24 hours before preparation of samples. Nitrates of lithium and cobalt were weighed according to cationic ratio to synthesis of $LiCoO_2$. Nitrates of nickel, lithium and cobalt were weighed according to cationic ratio to synthesis $LiCo_{0.4}Ni_{0.6}O_2$ , and made two separate solutions in ethyl alcohol ( 99.9% purity). The extensively mixed alcoholic solutions of lithium, or/and nickel (for preparation of $LiCo_{0.4}Ni_{0.6}O_2$) and cobalt nitrates, and citric acid (99.7% purity) solution were added to alcohol under constant stirring. The equivalent volume amount of acid to metal ions ratio was used. Thoroughly mixed alcoholic solutions of nitrates were heated under constant stirring at 80 °C for 2 h, to make the mixture denser and to form 'sol'. The 'sol' was then heated at 120 °C until a gel was formed and subsequently vacuum dried. The dried mass was collected and subjected to a further heat treatment at 800 °C for 12 h in air to obtain $LiCoO_2$ and $LiCo_{0.4}Ni_{0.6}O_2$ respectively. The characteristics of the compounds were studied using XRD, FTIR and DSC.

The synthesized compound, 10% of acetylene black and 15% of PVDF were dissolved in DBP (Dibutyl Phthalate) for making composite electrode. The slurry was applied uniformly on a thin polythene sheet and dried under vacuum. Thin circular membranes

were cut from the film and mounted in a coin type (CR2430) cell, with metallic lithium as the counter and reference electrodes, and Celgard 2400 membrane as the separator. A solution of 1M $LiPF_6$ in EC/ DMC with 1:1 by volume prepared in an argon-filled glove box was used as the liquid electrolyte in the cell. The cell properties were measured with a MacPile potentiostat-galvanostat instrument. After the electrochemical test, the changes to the structure of the $LiCoO_2$ and $LiCo_{0.4}Ni_{0.6}O_2$ cathode materials were tested using XRD.

Lithium-ion cells were assembled with synthesized materials as composite cathode and vein graphite as composite anode. Other components and preparation method were same as above.

## 3. RESULTS AND DISCUSSION

### 3.1 Structural Analysis

X ray diffractograms of the $LiCoO_2$ and $LiCo_{0.4}Ni_{0.6}O_2$ materials synthesized by sol-gel process are shown in Fig.1. According the XRD pattern the complete formation of impurity free $LiCoO_2$ but for the $LiCo_{0.4}Ni_{0.6}O_2$ sample $Co_2O_3$ peaks can be observed as an impurity.

All the X-ray peaks could be indexed by assuming a hexagonal lattice structure of the $\alpha$-$NaFeO_2$ type. The unit cell lattice parameters $a$ and $c$ of the cathode materials are listed in table 1.
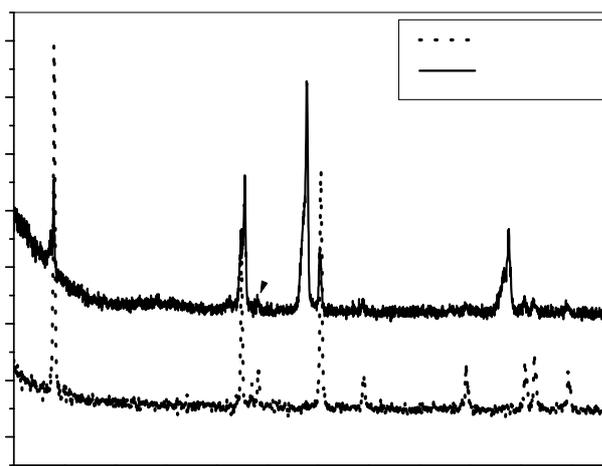


Figure 1:  X ray diffractograms of the $LiCoO_2$ and $LiCo_{0.4}Ni_{0.6}O_2$ materials synthesized by sol-gel process.  A peak due to trace impurity of $Co_2O_3$ is indicated.

As the intensity ratio $I_{(003)}/I_{(104)}$ is a key parameter indicating the degree of occupation of nickel ions in lithium predominating layers. There is a clear splitting of the (006) - (012)

and (018) - (110) doublet peaks which is a qualitative indication of an ordered distribution of lithium and transition metal ions in the lattice of $LiCoO_2$ and $LiCo_{0.4}Ni_{0.6}O_2$.

Table 1: Variation of unit cell parameters of the synthesized cathode materials

| Material | Structural data | | | | |
|---|---|---|---|---|---|
| | Space group | $a$ (Å) | $c$ (Å) | $c/a$ | RIR $(I_{(003)}/I_{(104)})$ |
| $LiCoO_2$ | Rhombohedral (Hexa.) R3m | 2.831 | 14.008 | 4.948 | 1.422 |
| $LiCo_{0.4}Ni_{0.6}O_2$ | Rhombohedral (Hexa.) R3m | 2.832 | 14.058 | 4.964 | 1.726 |

The relative intensity ratio (RIR) of (003) and (104) peaks and/or RIR of (101)/ (012, 006) are considered to be indications of the ordering of lithium and transition metal [5]. The lattice parameters of synthesized $LiCoO_2$ are comparable to the JCPDS (50-653) index values of $a$ = 2.81498 Å and $c$ = 14.0493 Å. Fig. 2 also shows that the relative intensity ratio of (003) and (104) peaks in the $LiCoO_2$ is higher than in theoretical ratio 0.87 by assuming complete occupation of transition metals.

The lattice parameter $a$ of $LiCo_{0.4}Ni_{0.6}O_2$ is similar to the reported value in the JCPDS (50-509) index but parameter $c$ is slightly higher than the value of the commercial lithium nickel cobalt oxide value of $c$ = 13.91 Å. The relative intensity ratio of (003) and (104) peaks synthesized material is about 45% higher than the theoretical ratio of 1.1765. The other important features of these layered-type compounds are the well defined doublets in our case (006, 012) and (018, 110).
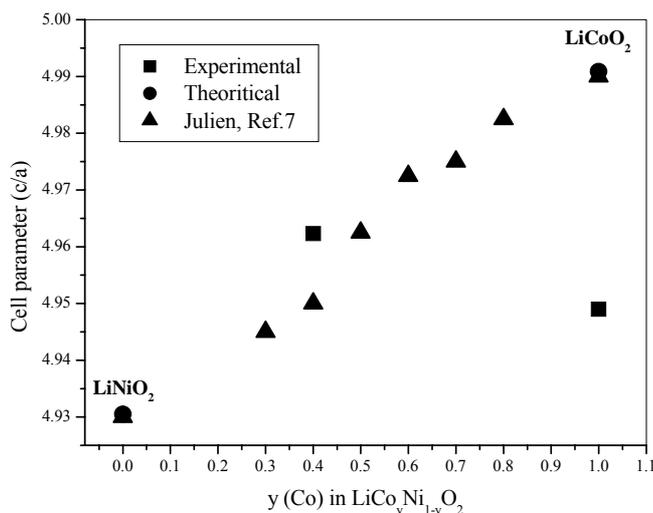


Figure 2: The variation of hexagonal unit-cell parameters with cobalt concentration y in $LiCo_yNi_{1-y}O_2$

Fig. 2 shows that the cell constant (*c/a*) of $LiCo_yNi_{(1-y)}O_2$ $(0 \leq y \leq 1)$ was prepared by sol-gel method mixing of acetates of the metals, Ni and Co, with the chelating agent, citric acid, in an aqueous medium [6], and our experiments results. The evolution of the crystallographic parameters as a function of cobalt composition in $LiCo_yNi_{(1-y)}O_2$ powders show that the cobalt rich compounds have the smaller parameters because $Co^{+3}$ (0.685 Å) has a smaller ionic radius than $Ni^{3+}$ (0.70 Å).

## 3.2 Spectroscopic studies

FTIR spectroscopy is capable of probing directly the surrounding environment of the cation (lithium ion) and the unique fingerprint of the Li site occupancy in the $\alpha$-$NaFeO_2$ type structures such as $LiCoO_2$ and $LiCo_yNi_{(1-y)}O_2$ [1]. Factor group analysis of the layered oxide, predicts four IR- active $(2A_{2u} + 2E_u)$ and two Raman active $(A_{1g} + E_g)$ vibrational modes.

Among the four IR-active modes, three bonds are in 400-600 $cm^{-1}$ region corresponding to $CoO_6$ stretching and bending vibrations while the fourth is a low-frequency band situated at 250-270 $cm^{-1}$ corresponding to $LiO_6$ vibrations [7-9]. Fig. 3 shows that the FTIR optic density spectrum of $LiCoO_2$ indicates the IR bands for $LiCoO_2$ at 270, 510, 600 and 640 $cm^{-1}$ whereas Julien [7] identified the IR bands of $LiCoO_2$ at 269, 418, 539 and 602 $cm^{-1}$ as well as Huang & Frech [5] reported bands at 271, 537, 595 and 653 $cm^{-1}$ for the same compound. The very high frequency band of the FTIR absorption spectrum of $LiCoO_2$ located at 1028 $cm^{-1}$ is attributed to the asymmetric stretching modes of CoO2.
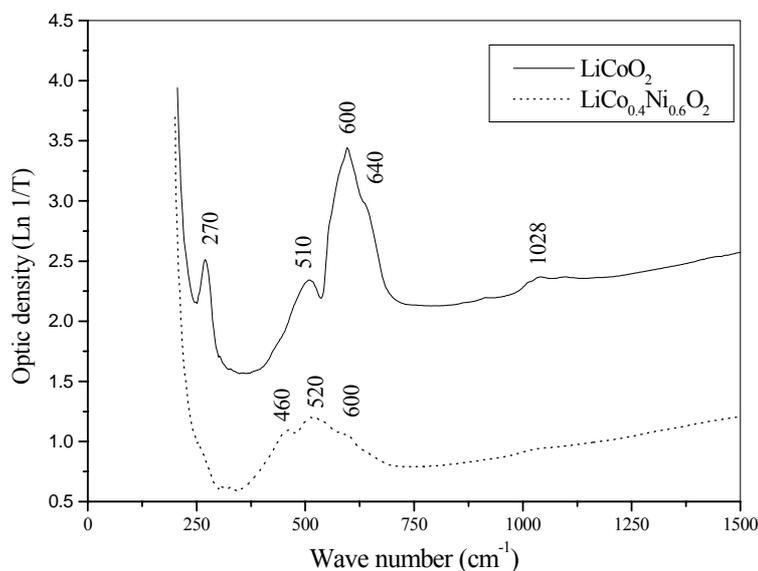
Figure 3: FTIR spectra of $LiCoO_2$ and $LiCo_{0.4}Ni_{0.6}O_2$ compounds prepared by sol-gel synthesis method using citric acid as a chelating agent.

The frequency shift of both stretching and bending modes as a function of the cobalt substitution leads to the cationic disorder in the $Co_yNi_{(1-y)}O_2$ slabs [7]. The frequency shift of the $LiO_6$ mode is attributed to slight change of the inter slab distance ($c_{hex}$ cell parameter) and the small mixing of Li-O stretching and O-M-O bending motion present in the low frequency range. Fig. 3 also shows that the FTIR optic density spectrum of $LiCo_{0.4}Ni_{0.6}O_2$ indicates only three peaks at 460, 520 and 600 $cm^{-1}$ in higher frequency range. The broadening of the high frequency range of IR bands is related with a non–homogenous Ni/Co distribution, variation in the Cobalt-anion bond lengths, and /or polyhedral distortion occurring in $LiCo_yNi_{(1-y)}O_2$ [7].

The DSC-TG results for the $LiCoO_2$ and $LiCo_{0.4}Ni_{0.6}O_2$, the first weight loss begins at about 120 °C and 180 °C. The weight loss at 180 °C is about 15% and 7% for $LiCoO_2$ and $LiCo_{0.4}Ni_{0.6}O_2$ respectively. The associated endothermic effect losses are attributed to removal of residual water and alcohol. The second step starts from 180 °C to 300 °C for both materials. After the removal of the remaining water molecules, the weight loss at 300 °C is 54.5% and 26% for $LiCoO_2$ and $LiCo_{0.4}Ni_{0.6}O_2$ respectively.



(a)                               (b)
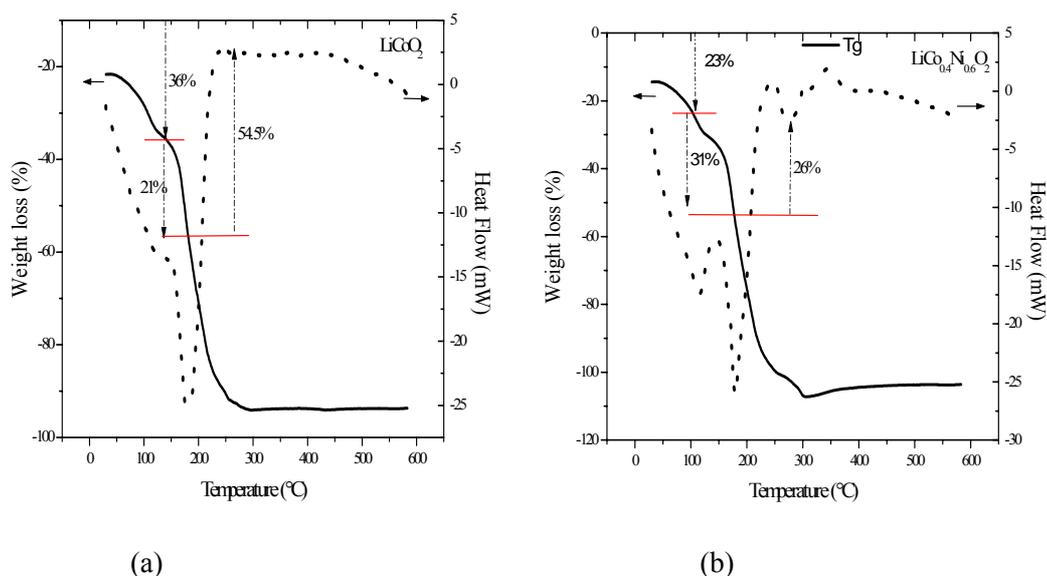
Figure 4:   TG-DTA data of the $LiCoO_2$ (a) and $LiCo_{0.4}Ni_{0.6}O_2$ (b) oxides grown by citric acid-assisted sol gel method. TG (full line), DTA (dotted line).

## 3.3 Cyclic voltammetry

Cyclic voltammetry is a more sensitive technique for the detection of phase transformations and that of non-uniform distribution of metal ions in the crystals lattice: or presence of a second phase as compared to powder XRD [10-11]. Fig. 5(a) shows that the cyclic voltammograms of $LiCoO_2$ indicate the voltage range of lithium deintercalation/ intercalation as well as the phase transitions of the compounds during the process. The first cycle of anodic curve shows two distinct peaks, one broad peak at 4.00 V - 4.15 V vs. $Li/Li^+$, indicating a single phase deintercalation reaction and another peak at 4.20 V

corresponding to the hexagonal to monoclinic phase transition. The anodic peaks are very thin at 4.20 V whereas the cathodic scan of the deintercalation shows a kink at 4.15 V which indicates a restructuring of the ions in the lattice (second order phase transition).

Fig. 5(b) shows that the cyclic voltammogram of $LiCo_{0.4}Ni_{0.6}O_2$ shows that as the main anodic and cathodic peak voltages decrease, the area under the curves also decreases lowering the incremental specific capacity to 50-60 A h $kg^{-1}$, indicating a poor reversibility of the electrode.



(a)                                              (b)
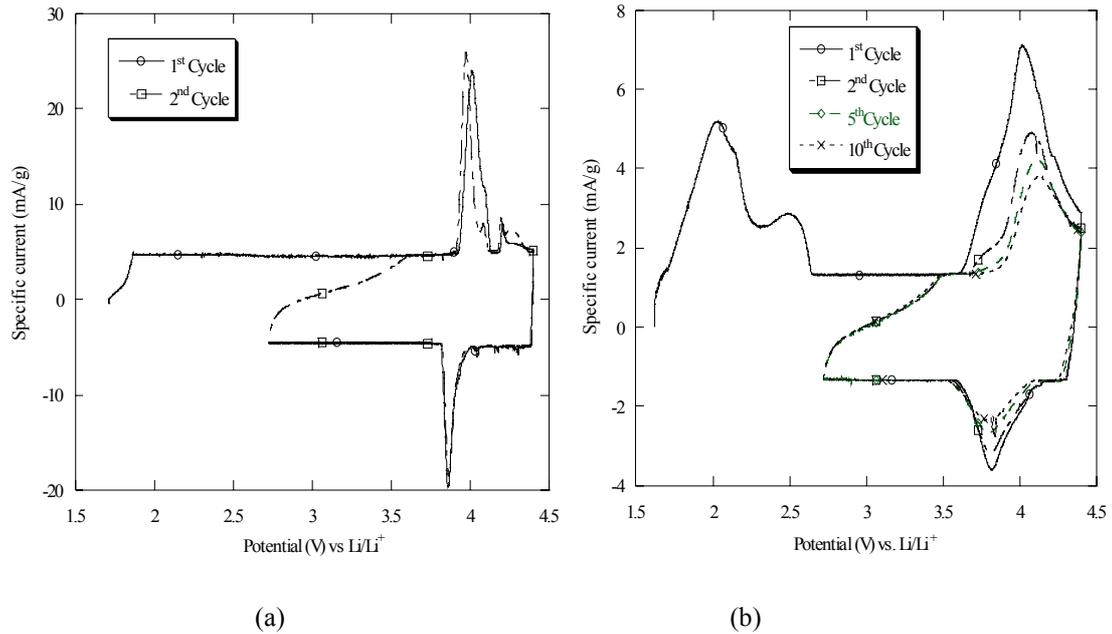
Figure 5:    Cyclic voltamograms (a) $LiCoO_2$ in coin type cell with Li/ $LiCoO_2$ at scan rate, 8µV/s and  (b)
$LiCo_{0.4}Ni_{0.6}O_2$ in coin type cell with Li/ $LiCo_{0.4}Ni_{0.6}O_2$ at scan rate, 32 µV $s^{-1}$ .

The main anodic and cathodic peak voltages decreases and the peaks become sharper, indicating better reversibility of the electrode. It can be concluded that reversible Li deintercalation/intercalation is possible in $LiCoO_2$ in the 2.75 V- 4.40 V voltage range. However, phase transformation from hexagonal to monoclinic phase, occurring between 4.10 V and 4.20 V vs. Li/Li$^+$ , induces a non-uniform volume change along the `c´ direction, due to strains and extended defects (micro cracks) between and within the particles, resulting in increased cell capacity fading [12].

### 3.4 Galvanostatic charge-discharge

In order to study the electrochemical performance of $LiCoO_2$ and the effect of Ni substitution on the deintercalation voltage of $LiCoO_2$, the galvanostatic charging and discharging at slow current rate of 5 and 10 A $kg^{-1}$ for Li/$LiCoO_2$ and Li/ $LiCo_{0.4}Ni_{0.6}O_2$ cells with charge cutoff voltage of 4.40 V and a discharge cutoff voltage of 2.75 V were performed. Table 2 shows The irreversible capacity loss of $LiCoO_2$ during the first-charge-discharge is about 20% and for $LiCo_{0.4}Ni_{0.6}O_2$ is about 90%.  For the compound of

$LiC_{0.4}Ni_{0.6}O_2$, the first discharge capacities decreased drastically and found that negligible amounts of lithium could be extracted electrochemically. This behavior is as expected from their cyclic voltammetric results indicating the prepared material is in impure.

Table 2: Variation of cathodic capacity for the first cycle of the cathode materials at different current rates

| Material | Cathodic capacity (A h kg$^{-1}$) | | | |
|---|---|---|---|---|
| | Current rate (A kg$^{-1}$) | 1$^{st}$ charge | 1$^{st}$ discharge | 1$^{st}$ irreversible % |
| $LiCoO_2$ | 5 | 192 | 155 | 19 |
| | 10 | 158 | 135 | 15 |
| $Li\,Co_{0.4}Ni_{0.6}O_2$ | 5 | 122 | 15 | 88 |
| | 10 | 207 | 19 | 91 |

The charge –discharge curves in the voltage range of 2.75 V and 4.40 V at a current rate of 10 A kg$^{-1}$, obtained for $LiCoO_2$ and $LiCo_{0.4}Ni_{0.6}O_2$ cathode materials synthesized by sol-gel methods showing in Fig.6. The shape of the charge-discharge curve of $LiCoO_2$ shows a good reversibility.



(a)                                    (b)
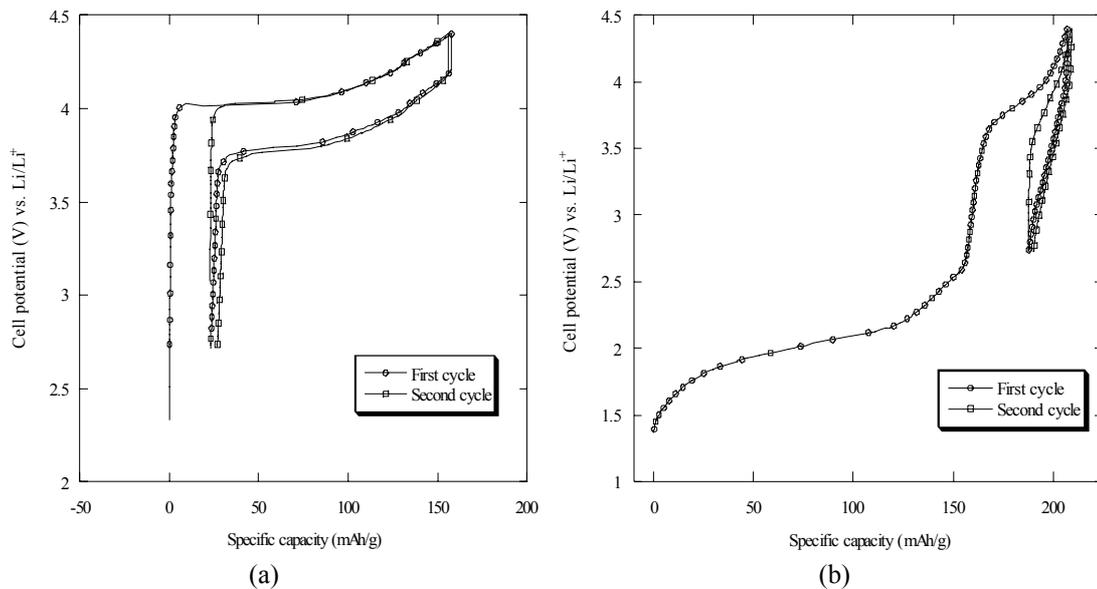
Figure 6:  Voltage profiles of coin type cell with Li/ $LiCoO_2$ (a) and Li/ $LiCo_{0.4}Ni_{0.6}O_2$ (b) at a current  rate of 10 A kg$^{-1}$

However, Fig. 6 also shows that the fully intercalated phase of $LiCo_{0.4}Ni_{0.6}O_2$ is not recovered during the first discharge and found very poor cycleability. This could be probably assigned to a kinetic problem especially as the $LiCo_{0.4}Ni_{0.6}O_2$ phases are poor electronic conductors. The plateau at 4.25 V is attributed to oxidation of $Co^{3+}$ ions but the charge- discharge curve of $LiCo_{0.4}Ni_{0.6}O_2$ does not show to oxidation of $Ni^{3+}$. Generally, oxidation of $Ni^{3+}$ ions is prior to oxidation of $Co^{3+}$ [13].

Fig. 7(a) shows the variation of the discharge capacity of Li/$LiCoO_2$ cells during the first 15 cycles of cells, cycled between 2.75 V to 4.40 V vs. Li/Li$^+$. It is worth noticing here

that, despite the fairly low current density utilized (5 A kg$^{-1}$), the value of the specific capacity cycled is still about 90% of the theoretical value after 15 cycles. Overall capacity retention of the material is quite good.
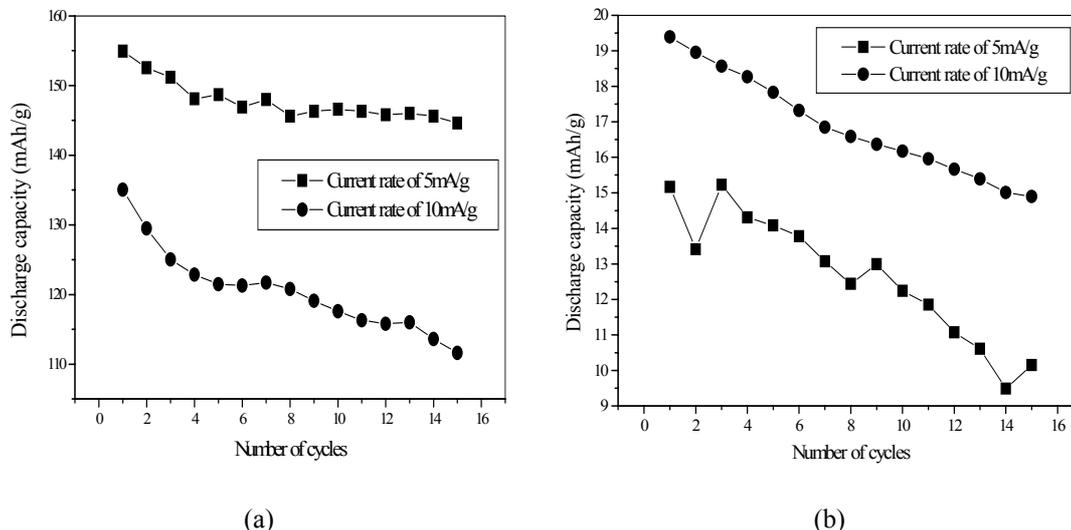


Figure 7: Discharge capacity versus. Number of cycles of charge-discharge cycles for the compound, LiCoO$_2$ (a) and LiCo$_{0.4}$Ni$_{0.6}$O$_2$ (b) at different current rates. Voltage window: 2.75-4.40 V.

Fig. 7 also shows that the discharge capacity values for LiCoO$_2$ are consistently higher than of LiCo$_{0.4}$Ni$_{0.6}$O$_2$ compound. The capacity retention, as a percentage of the initial discharge capacity is about 155 and 135 A h kg$^{-1}$ at slow current rates of 5 and 10 A kg$^{-1}$ for LiCoO$_2$ at and decreases from 7% to 17% for the 15$^{th}$ cycle, indicating smaller capacity fading for the latter.

## 3.5  XRD studies after cycling

The XRD is performed in order to observe any structural changes induced during the electrochemical charge-discharge cycling. The unit cell lattice parameters, `*a*´ and `*c*´, of the cathode materials after 15 cycles, listed in table 3.

Table 3: Variation of unit cell parameters of the cathode materials after 15 cycles at current rate, 10mA/g

| Material | Structural data | | | |
|---|---|---|---|---|
| | a (Å) | c (Å) | c/a | RIR ($I_{(003)}/I_{(104)}$) |
| LiCoO$_2$ | 2.845 | 14.505 | 5.099 | 2.415 |
| LiCo$_{0.4}$Ni$_{0.6}$ O$_2$ | 2.874 | 14.40 | 5.010 | 1.863 |

This is a clear indication of the cation-mixing occurring in the Li and Co/Ni layers during cycling. However, complete cation-mixing does not occur since the (006, 012) and (018, 110) doublet peaks are clearly discernable.

Fig.8 shows that the X-ray patterns of the $LiCoO_2$ and $LiCo_{0.4}Ni_{0.6}O_2$ cathodes before and after 15 cycles between 2.75 and 4.40 V vs. $Li/Li^+$ at current rate, 10 A $kg^{-1}$. As can be seen the layered $NaFeO_2$ structure is retained in both the compounds. However, the diffraction lines of the cycled cathodes broadened and more diffused as compared to before cycling for a given composition. Since composite electrode is strongly orientated in the (003) direction, it is impossible to detect any change in the diffraction patterns. Changes of lattice constant *c/a*, of the both materials increased after cycling, indicating that lattice expands preferentially in the direction of the *c*-axis.



(a)                                                        (b)
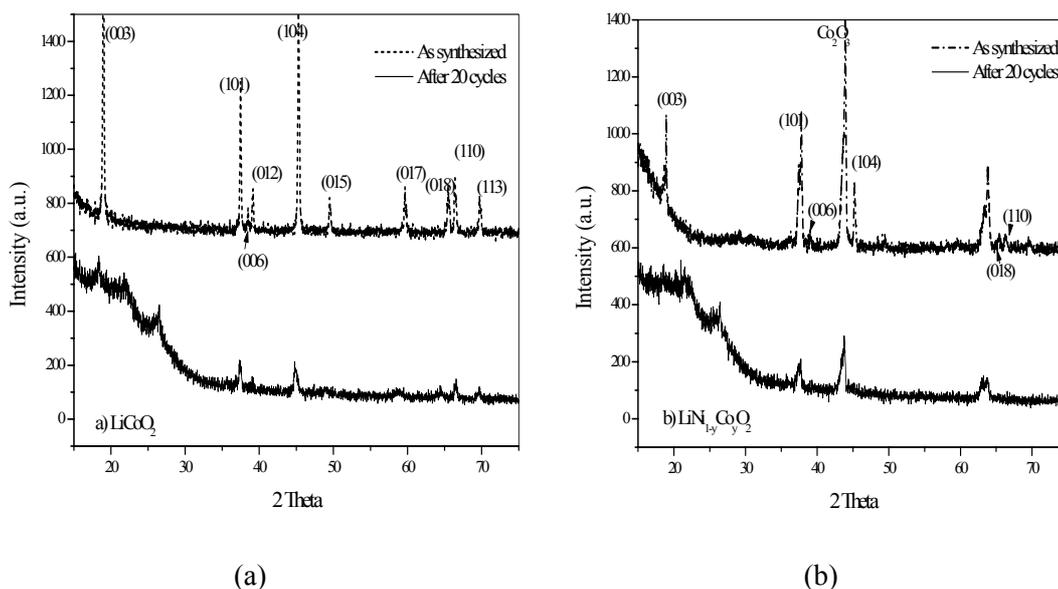
Figure 8: Patterns of the $LiCoO_2$ (a) and $LiCo_{0.4}Ni_{0.6}O_2$ (b) cathodes before and after 20 cycles between 2.725 – 4.40 V at current density of 10mA/g. A peak due to trace impurity of $Co_2O_3$ is indicated.

## 3.6 Electrochemical performance of Li-ion batteries

The active materials in Li-ion batteries operate by reversibly incorporating lithium in an intercalation process. The synthesized $LiCo_{0.4}Ni_{0.6}O_2$ as cathode material and vein graphite as the anode material were performed in Li-ion batteries in our experiments. When a Li-ion battery is charged, the cathode material ($LiCo_{0.4}Ni_{0.6}O_2$) is oxidized and the anode material (graphite) is reduced. As metallic lithium is not present in the cell, Li-ion batteries are chemically less reactive, safer, and offer longer cycle life than possible with rechargeable lithium batteries that employ lithium metal as the negative electrode material. Fig. 9 shows that the overall capacity retention of the Li-ion batteries made using different types of natural graphite and synthesized cathode material are between 19% - 41%, indicating larger capacity fading during the progressing of cycles. It is noticed here that the overall capacity retention of the Li-ion batteries which are made using different types of natural graphite and cathode material, is not quite good.
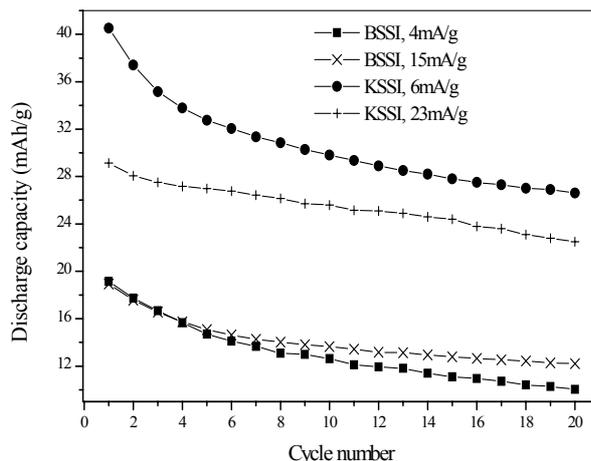
Figure 9: Discharge capacity of the Li-ion batteries at different current rates; $LiCo_{0.4}Ni_{0.6}O_2$ as a cathode material and BSSI and KSSI natural graphite composite electrode as an anode materials.

## 4. CONCLUSION

The sol-gel synthesized $LiCoO_2$ shows an interesting high reversible capacity for the lithium intercalation/deintercalation process and a good cycleability even at high anodic potential up to 4.40 V and then degradation processes usually occur. However fully intercalated phase of $LiCo_{0.4}Ni_{0.6}O_2$ is not recovered during the first discharge cycle due to the *s*-block or *p*-block metal substitution and a poor cycleability is observed due to impurity content. This could be probably due to a kinetic reason especially as the $LiCo_{0.4}Ni_{0.6}O_2$ phases are poor electronic conductors.

Furthermore, the $LiCoO_2$ cathode material has shown a quite interesting value of charge retention upon cycling. The specific capacity remains at about 90% of the theoretical value after more than 15 cycles. These results confirm the satisfactory electrochemical performance of the above material when operating as cathodes in Li-ion battery systems. This preparation method can be considered as a new route to form better cathode materials by changing variables in sol-gel synthesis which enhances both the purity, and even more importantly, the morphology of the powders.

## ACKNOWLEDGMENTS

## REFERENCES

1.  Y.S. Lee, Y.K. Sun and K.S. Nahm, *Synthesis and Characterization of LiNiO₂ Cathode Material Prepared by an Adiphic Acid-assisted Sol-gel Method for Lithium Secondary Batteries*, Solid State Ion., <u>118 </u>(1999), p.159.

2.  Y.D. Zhong, X.B. Zhao, G.S. Cao, J.P. Tu, T.J. Zhu, *Characterization of particulate sol-gel synthesis of LiNi₀.₈Co₀.₂O₂ via maleic acid assistance with different solvents*, J. Alloys and Compounds, <u>420</u> ( 2006), p.298.

3.  Y.K. Sun, *Synthesis and Electrochemical Studies of Spinel Li₁.₀₃Mn₂O₄ Cathode Materials Prepared by a Sol-gel Method for Lithium Secondary Batteries*, Solid State Ionics, <u>100</u> (1997), p.115.

4.  B. J Hwang, R. Santhanam and C.H. Chen, *Effect of Synthesis Conditions on Electrochemical Properties of LiNi₁₋ᵧCoᵧO₂ Cathode for Lithium Rechargeable Batteries*, J. Power Sources, <u>5059</u> (2002), p.1.

5.  W. Huang, R. Frech, *Vibrational spectroscopic and electrochemical studies of the low and high temperature phases of LiCo₁₋ₓ MₓO₂ (M = Ni or Ti)*, Solid State Ionics, <u>86-88</u> (1996), p.395.

6.  C. Julien, *Materials for Lithium – Ion Batteries*, edited by C. Julien, and Z. Stoynoc, (NATO Science Series, 1998), <u>3 (85)</u>, p.225.

7.  C. Julien, *4-Volt Cathode Materials for Rechargeable Lithium Batteries Wet –Chemistry Synthesis, Structure and Electrochemistry*, Ionics, <u>6</u> (2000), p.30.

8.  H. Arai, S. Okada, Y. Sakurai and J. Yamaki, *Thermal Behavior of Li₁₋ᵧNiO₂ and the Decomposition Mechanism*, Solid State Ionics, <u>109 </u>(1998), p.295.

9.  M. M. Rao, C. Liebenow, M. Jayalakshmi, H. Wulff, U. Guth and F. Scholz, *High-temperature Combustion Synthesis and Electrochemical Characterization of LiNiO₂, LiCoO₂ and LiMn₂O₄ for Lithium-ion Secondary Batteries*, J. Solid State Electrochem., <u>5</u> (2001), p.348.

10. W. Li, J. N. Reimers and J. R. Dahn, *Crystal Structure of LiₓNi₂₋ₓO₂ and a Lattice-gas Model for the Order-disorder Transition*, Phys. Rev. B, <u>46 </u>(1992), p.3236.

11. Y.M. Choi, S.I. Pyun, S.I. Moon and Y.E. Hyung, *A Study of the Electrochemical Lithium Intercalation Behavior of Porous LiNiO₂ Electrodes Prepared by Solid-state Reaction and Sol-gel Methods*, J. Power Sources, <u>72 </u>(1998), p.83.

12. J. N. Reimers, E. Rossen, C.D. Jones and J.R. Dahn, *Structure and Electrochemistry of LiₓFeᵧNi₁₋ᵧO₂*, Solid State Ionics, <u>61 </u>(1993), p.335.

13. G. T. K. Fey, V. Subramanian and J. G. Chen, *Synthesis of Non-stoichiometric Lithium Nickel Cobalt Oxides and Their Structural and Electrochemical Characterization*, Electrochem. Commun., <u>3</u> (2001), p.234.